PROCEEDINGS of the
23rd International Congress on Acoustics
9 to 13 September 2019 in Aachen, Germany

Non-iterative, conservative schemes for geometrically exact nonlinear string vibration

Michele DUCCESCHI[(1)], Stefan BILBAO[(1)]

[(1)]Acoutics and Audio Group, University of Edinburgh, UK, michele.ducceschi@ed.ac.uk

Abstract

This work presents novel finite difference schemes for the solution of the geometrically exact nonlinear model of wave propagation in strings. Stability is enforced by ensuring energy conservation in the discrete setting. The schemes are here derived from a suitable quadratisation of the nonlinear potential, yielding ultimately a non-iterative update equation requiring the solution of a sparse linear system per time step. Comparison with previous iterative schemes is carried out, showing convergence to a unique solution. The new schemes are extremely efficient, yielding speedups of about half an order of magnitude over previously available schemes.

Keywords: Finite Difference Schemes, Energy Methods, Nonlinear Wave Equation, Piano Acoustics

1 INTRODUCTION

Computer simulation of nonlinear phenomena is a subject of growing interest in acoustics and musical acoustics. Though linear models are adequate in many situations, exceptions are many: in one dimension, a nonlinear wave equation is required to fully capture the behaviour of piano strings, for instance. When it comes to simulation, the algorithm designer is faced with two main concerns: one is ensuring convergence of the schemes; the other is efficiency. Among the usual approaches in numerical simulation for nonlinear systems are iterative schemes, obtained via discretisation methods such as the bilinear transform (i.e. the trapezoid rule.) These techniques lead to stable and convergent schemes, but can be quite inefficient, especially when solving for distributed nonlinearities such as those occurring in a piano string. Recently, a new class of methods has been proposed, relying on a suitable quadratisation of the nonlinear potential energy. Such methods appeared first in virtual-analog simulation (1, 2, 3), and have been extended to include the case of non-invertible potentials (4, 5, 6), and here to the case of a fully distributed nonlinearity. Applications in fluid dynamics have also been devised (7). The proposed schemes ultimately lead to update equations which are resolvable without recourse to iterative methods, and which maintain the notion of an energy balance leading to a numerical stability guarantee. In Section 2 the continuous models of nonlinear string vibration are presented, along with considerations regarding the quadratisation of the potential, and a linear expansion. In Section 3 two conservative finite difference schemes are given: the first, iterative in nature, follows from a discretisation obtained via the trapezoid rule; the second is the newly proposed non-iterative scheme. Finally, in Section 4 some numerical experiments are detailed.

2 MODEL EQUATIONS

In musical acoustics, it is often assumed that a uniform string vibrates according to the simple wave equation. There are two cases when this assumption is no longer valid: when the string has intrinsic stiffness, and when it vibrates at higher amplitudes. Stiffness is indeed a prominent effect across all musical strings, and it can be incorporated by means of an appropriate linear beam model. From a numerical standpoint, it has been studied in numerous other works [see, e.g. (8, 9)], so here the focus will be exclusively on the second effect, nonlinearities. In the case of a string vibrating in isolation, these are of geometric type and arise when the vibration amplitude is large. It is in fact possible to derive a model which is geometrically exact, by calculating the extension of an infinitesimal string element under tension (10). Ultimately, the stretching of the string leads

to tension modulation (as opposed to the linear case, where tension is constant.) In vector form, this model is

$$\rho A \partial_t^2 \mathbf{w} = \partial_x \left(\nabla_{(q,p)} \Xi \right), \quad \text{with } \Xi(q,p) = \frac{EA}{2}\left(q^2+p^2\right) - (EA - T_0)\left(\sqrt{(1+p)^2+q^2} - 1 - p \right) \geq 0 \ \forall \ (q,p) \tag{1}$$

where Ξ is interpreted as a positive-definite potential function. Above, ρ is the volumetric density, and A is the area of the cross section, E is Young's modulus and T_0 is the applied tension. The string occupies a domain $x \in \mathscr{D} = [0, L]$. The symbol ∂_s^n denotes the n^{th} partial derivative along s, and $\nabla_{(q,p)}$ is the gradient taken along q and p. Assuming the motion to be constrained in a single plane, one can identify $\mathbf{w}(t,x) = {}^T[u(t,x), \zeta(t,x)]$, where u is the transverse (or vertical) displacement, and ζ is the longitudinal (or horizontal) displacement. Hence, $q \triangleq \partial_x u$ and $p \triangleq \partial_x \zeta$. It is convenient to rewrite (1) in a different, yet equivalent form, as

$$\rho A \partial_t^2 u = T_0 \partial_x^2 u + \partial_x(\partial_q \phi) \tag{2a}$$

$$\rho A \partial_t^2 \zeta = T_0 \partial_x^2 \zeta + \partial_x(\partial_p \phi) \tag{2b}$$

where

$$\phi = \frac{EA - T_0}{2}\left(\sqrt{(1+p)^2+q^2} - 1 \right)^2 \tag{3}$$

Notice that ϕ is positive definite, if $EA > T_0$ (certainly the case for all musical strings.)

2.1 Inner product and energy analysis in the continuous case

An energy analysis of (2) is readily available upon the introduction of an inner product and associated norm. For two well-behaved functions c, d, one has

$$\text{Inner Product: } \langle c, d \rangle_{\mathscr{D}} = \int_0^L c\, d \, \mathrm{d}x, \qquad \text{Norm: } \|c\|_{\mathscr{D}} = \sqrt{\langle c, c \rangle_{\mathscr{D}}} \tag{4}$$

Taking an inner product of (2a) with $\partial_t u$, and of (2b) with $\partial_t \zeta$ gives (after integration by parts)

$$\frac{\mathrm{d}\mathfrak{H}}{\mathrm{d}t} = \mathfrak{B} \tag{5}$$

with $\mathfrak{H}$ being the total energy, and with $\mathfrak{B}$ being the boundary conditions. The analytic expressions are

$$\mathfrak{H} = \frac{\rho A}{2}\left(\|\partial_t u\|_{\mathscr{D}}^2 + \|\partial_t \zeta\|_{\mathscr{D}}^2 \right) + \frac{T_0}{2}\left(\|q\|_{\mathscr{D}}^2 + \|p\|_{\mathscr{D}}^2 \right) + < \phi, 1 >_{\mathscr{D}} \tag{6a}$$

$$\mathfrak{B} = \left[\partial_t u \left(T_0 q + \partial_q \phi \right) + \partial_t \zeta \left(T_0 p + \partial_p \phi \right) \right]_0^L \tag{6b}$$

A convenient set of boundary conditions which make $\mathfrak{B}$ vanish, used in this work, is then

$$u = \zeta = 0 \text{ at } x = 0, L \tag{7}$$

2.2 Quadratisation of the nonlinear potential

A convenient alternate form of the equations of motion can be derived by quadratising the potential ϕ. Hence, take

$$\psi = \sqrt{2\phi} \tag{8}$$

One has

$$\rho A \partial_t^2 u = T_0 \partial_x^2 u + \partial_x(\psi \partial_q \psi) \tag{9a}$$

$$\rho A \partial_t^2 \zeta = T_0 \partial_x^2 \zeta + \partial_x(\psi \partial_p \psi) \tag{9b}$$

The energy analysis in this case yields an energy balance analogous to (5), where now

$$\mathfrak{H} = \frac{\rho A}{2}\left(\|\partial_t u\|_{\mathscr{D}}^2 + \|\partial_t \zeta\|_{\mathscr{D}}^2 \right) + \frac{T_0}{2}\left(\|q\|_{\mathscr{D}}^2 + \|p\|_{\mathscr{D}}^2 \right) + \frac{\|\psi\|_{\mathscr{D}}^2}{2} \tag{10a}$$

$$\mathfrak{B} = \left[\partial_t u \left(T_0 q + \psi \partial_q \psi \right) + \partial_t \zeta \left(T_0 p + \psi \partial_p \psi \right) \right]_0^L \tag{10b}$$

Though (9) and (2) are completely equivalent (so long as ψ is well defined, i.e. so long as, from (8), ϕ is non-negative), the two forms lead to very different discrete methods: system (2) will require a nonlinear iterative root finder, whereas system (9) will be calculated by means of a simple matrix inversion.

2.3 Small oscillations and natural wave speeds

One may wonder what the behaviour of the nonlinear wave equation (2) is under small amplitudes. An expansion of ϕ to second order yields

$$\phi \approx \frac{EA - T_0}{2} p^2 \tag{11}$$

Inserting this value in (2) gives

$$\rho A \partial_t^2 u = T_0 \partial_x^2 u \tag{12a}$$

$$\rho A \partial_t^2 \zeta = EA \partial_x^2 \zeta \tag{12b}$$

Hence, for small amplitudes, the system is completely uncoupled, and both transverse and longitudinal motions are given by the linear wave equation with speeds, respectively, $v_u = \sqrt{T_0/\rho A}$ and $v_\zeta = \sqrt{E/\rho}$. Notice that for musical strings, normally $v_\zeta \gg v_u$, and this will have consequences in terms of the choice of the grid spacing in the finite difference schemes.

3 DISCRETE MODEL

Solutions to the nonlinear wave equation are sought by means of the finite difference method. The continuous functions $u(t,x)$, $\zeta(t,x)$ are approximated by grid functions $u_m^n \triangleq u(nk,mh)$, $\zeta_m^n \triangleq \zeta(nk,mh)$, where the indices m,n are positive integers, and where k is the time step, and h is the grid spacing. It is assumed that $n \geq 0$ and $m \in \mathbb{M} = [0,M]$, and thus the grid spacing h divides the domain length L in M equal intervals. The continuous functions $p(t,x), q(t,x)$ are approximated by $p_{m-1/2}^n$, $q_{m-1/2}^n$, defined on an interleaved spatial grid $m \in \mathbb{M} = [1,M]$. In the following, in order to keep the index notation to a minimum, it will be assumed that the notation u stands for u_m^n, and similarly for ζ, p and q (these last two defined on an interleaved grid.) Indices will be specified only when needed.

Finite difference operators are now introduced. The identity and time shifting operators are

$$1 w_m^n = w_m^n, \quad e_{t+} w_m^n = w_m^{n+1} \quad e_{t-} w_m^n = w_m^{n-1} \tag{13}$$

Time difference operators may be introduced as

$$\delta_{t+} \triangleq \frac{e_{t+} - 1}{k}, \quad \delta_{t-} \triangleq \frac{1 - e_{t-}}{k}, \quad \delta_{t\cdot} \triangleq \frac{e_{t+} - e_{t-}}{2k}, \quad \delta_{tt} \triangleq \delta_{t+}\delta_{t-} \tag{14}$$

Time averaging operators are

$$\mu_{t+} \triangleq \frac{1 + e_{t+}}{2}, \quad \mu_{t-} \triangleq \frac{1 + e_{t-}}{2}, \quad \mu_{t\cdot} \triangleq \frac{e_{t+} + e_{t-}}{2} \tag{15}$$

Space shifting operators are defined as

$$e_{x+} w_m^n = w_{m+1}^n, \quad e_{x-} w_m^n = w_{m-1}^n \tag{16}$$

Similar definitions hold for spacial operators acting on an interleaved grid function. From those, space difference operators are given as

$$\delta_{x+} \triangleq \frac{e_{x+} - 1}{h}, \quad \delta_{x-} \triangleq \frac{1 - e_{x-}}{h}, \quad \delta_{xx} \triangleq \delta_{x+}\delta_{x-} \tag{17}$$

Partial differentiation of the potential ϕ with respect to p,q is given as

$$\delta_{q\cdot}\phi(q^n,p^n) \triangleq \frac{\phi(q^{n+1},p^n) - \phi(q^{n-1},p^n)}{q^{n+1} - q^{n-1}}, \quad \delta_{p\cdot}\phi(q^n,p^n) \triangleq \frac{\phi(q^n,p^{n+1}) - \phi(q^n,p^{n-1})}{p^{n+1} - p^{n-1}} \tag{18}$$

A particular averaging of ϕ will also be needed. This is

$$\mu_{q_-|p_-}\phi(q^n,p^n) \triangleq \frac{\phi(q^{n-1},p^n)+\phi(q^n,p^{n-1})}{2} \tag{19}$$

For two grid functions c_m, d_m defined over $\mathbb{D} = d_- \leq m \leq d_+$ one can define an inner product and associated norm, in analogy to (4), as

$$\text{Inner Product: } \langle c,d\rangle_{\mathbb{D}} = \sum_{m=d_-}^{d_+} h\, c_m\, d_m, \qquad \text{Norm: } \|c\|_{\mathbb{D}} = \sqrt{\langle c,c\rangle_{\mathbb{D}}} \tag{20}$$

3.1 Iterative, conservative scheme

A discretisation of (2) can be written as

$$\rho A\delta_{tt}u = T_0\delta_{xx}u + \delta_{x+}(\delta_{q\cdot}\phi) \tag{21a}$$

$$\rho A\delta_{tt}\zeta = T_0\delta_{xx}\zeta + \delta_{x+}(\delta_{p\cdot}\phi) \tag{21b}$$

where $q \triangleq \delta_{x-}u$, $p \triangleq \delta_{x-}\zeta$. This discretisation follows from applying the trapezoid rule to the nonlinear potential. An energy conservation property can be found by taking an inner product of (21a) with $\delta_{t\cdot}u$, and of (21b) with $\delta_{t\cdot}\zeta$, and by summing the resulting equations. Applying summation by parts gives

$$\delta_{t+}\mathfrak{h}^{n-1/2} = \mathfrak{b} \tag{22}$$

where

$$\mathfrak{h}^{n-1/2} = \frac{\rho A}{2}\left(\|\delta_{t-}u^n\|^2_{\mathbb{M}} + \|\delta_{t-}\zeta^n\|^2_{\mathbb{M}}\right) + \frac{T_0}{2}\left(\langle q^n, e_{t-}q^n\rangle_{\underline{\mathbb{M}}} + \langle p^n, e_{t-}p^n\rangle_{\underline{\mathbb{M}}}\right) + \left\langle 1, \mu_{q_-|p_-}\phi^n\right\rangle_{\underline{\mathbb{M}}} \tag{23}$$

and where the boundary term $\mathfrak{b}$ vanishes under a choice of fixed end conditions, i.e. $u_0 = u_M = \zeta_0 = \zeta_M = 0\ \forall n$. Notice that (22) is discrete version of (5). However, as opposed to the continuous energy $\mathfrak{H}$ which is always non-negative, the discrete energy $\mathfrak{h}$ in (23) will be non-negative if and only if (11)

$$h \geq \sqrt{\frac{T_0}{\rho A}}k \triangleq h^{(t)} \tag{24}$$

Non-negativity of the energy function assures stability and convergence for scheme (21).

Remark. Though condition (24) leads to stable simulations, choosing h to be close to $h^{(t)}$ would lead in this case to some aliasing problems. Remembering the linear expansion (12b), the natural grid spacing for the longitudinal grid is indeed $h^{(l)} = \sqrt{E/\rho}k$, which is much larger than $h^{(t)}$. In order to avoid such spacial sampling problems, in the following the choice $h = h^{(l)}$ will be enforced, along with frequency oversampling. More efficient schemes, avoiding oversampling, may be devised by interpolating between the longitudinal and transverse grids. However, this possibility will not be explored here, as the focus is only on the convergence and stability properties of the schemes ■

Both (21a) and (21b) can conveniently be multiplied on the left by δ_{x-}. This yields the following two equations

$$\rho A\delta_{tt}q = T_0\delta_{xx}q + \delta_{xx}(\delta_{q\cdot}\phi) \tag{25a}$$

$$\rho A\delta_{tt}p = T_0\delta_{xx}p + \delta_{xx}(\delta_{p\cdot}\phi) \tag{25b}$$

Then, define

$$r_{(q)} = q^{n+1} - q^{n-1}, \quad r_{(p)} = p^{n+1} - p^{n-1}, \quad a_{(q)} = q^{n-1}, \quad a_{(p)} = p^{n-1} \tag{26}$$

Owing to these definitions, one may recast system (25) in the following form

$$\frac{\rho A}{k^2}\left(r_{(q)}-2q^n+2q^{n-1}\right)=T_0\delta_{xx}q^n+\delta_{xx}\left(\frac{\phi\left(r_{(q)}+a_{(q)},p^n\right)-\phi\left(a_{(q)},p^n\right)}{r_{(q)}}\right)$$
$$\frac{\rho A}{k^2}\left(r_{(p)}-2p^n+2p^{n-1}\right)=T_0\delta_{xx}p^n+\delta_{xx}\left(\frac{\phi\left(q^n,r_{(p)}+a_{(p)}\right)-\phi\left(q^n,a_{(p)}\right)}{r_{(p)}}\right)$$

This form of the equations allows to solve for the unknowns $r_{(q)}, r_{(p)}$, using a convenient iterative root finder, such as Newton-Raphson. Existence and uniqueness of the solution may be proven by using convexity of ϕ, however the proof will be omitted here. The displacements u, ζ can be recovered from $r_{(q)}, r_{(p)}$ by solving the following linear systems

$$\delta_{x-}u^{n+1}=r_{(q)}+\delta_{x-}u^{n-1},\qquad \delta_{x-}\zeta^{n+1}=r_{(p)}+\delta_{x-}\zeta^{n-1} \tag{27}$$

3.2 Novel non-iterative, conservative scheme

A discretisation of (9) follows as

$$\rho A\delta_{tt}u=T_0\delta_{xx}u+\delta_{x+}\left(\left(\mu_{t+}\psi\right)g\right) \tag{28a}$$
$$\rho A\delta_{tt}\zeta=T_0\delta_{xx}\zeta+\delta_{x+}\left(\left(\mu_{t+}\psi\right)f\right) \tag{28b}$$

Above, it is understood that $\psi=\psi^{n-1/2}_{m-1/2}$, $g=g^n_{m-1/2}$ and $f=f^n_{m-1/2}$. The system is completed by an extra equation, relating the time derivative of ψ to f, g, as

$$\delta_{t+}\psi=g\delta_{t\cdot}q+f\delta_{t\cdot}p \tag{29}$$

Finally, g and f are calculated as the analytic derivatives of ψ with respect to p, q, at the current time step, i.e.

$$g^n_{m-1/2}=\partial_q\psi\Big|_{p=p^n_{m-1/2},q=q^n_{m-1/2}},\qquad f^n_{m-1/2}=\partial_p\psi\Big|_{p=p^n_{m-1/2},q=q^n_{m-1/2}} \tag{30}$$

Energy conservation can be shown once more by taking taking an inner product of (28a) with $\delta_{t\cdot}u$, and of (28b) with $\delta_{t\cdot}\zeta$. Summing the two resulting equations, and making use of (29) gives again an energy balance of the form (22), where in this case

$$\mathfrak{h}^{n-1/2}=\frac{\rho A}{2}\left(\|\delta_{t-}u^n\|^2_{\mathbb{M}}+\|\delta_{t-}\zeta^n\|^2_{\mathbb{M}}\right)+\frac{T_0}{2}\left(\langle q^n,e_{t-}q^n\rangle_{\underline{\mathbb{M}}}+\langle p^n,e_{t-}p^n\rangle_{\underline{\mathbb{M}}}\right)+\frac{\left\|\psi^{n-1/2}\right\|^2_{\underline{\mathbb{M}}}}{2} \tag{31}$$

and where the boundary term vanishes under the same fixed end conditions as before. Inspection of the energy function allows to write the same stability condition as (24), but as pointed out in the remark in section 3.1, the natural longitudinal grid spacing $h^{(l)}$ will be enforced here, to avoid aliasing.

Using the identity

$$\mu_{t+}\psi^{n-1/2}=\frac{k}{2}\delta_{t+}\psi^{n-1/2}+\psi^{n-1/2} \tag{32}$$

into (28a), (28b), and owing to (29), scheme (28) can be cast in a convenient matrix-vector update of the form

$$\mathbf{A}\mathbf{w}^{n+1}=\mathbf{b} \tag{33}$$

where $\mathbf{w}^{n+1}\triangleq{}^T[\mathbf{u}^{n+1},\boldsymbol{\zeta}^{n+1}]$ and where

$$\mathbf{A}=\begin{pmatrix}\frac{\rho A}{k^2}\mathbf{I}-\frac{1}{4}\mathbf{D}_x^+\boldsymbol{\Lambda}_{g^2}\mathbf{D}_x^- & -\frac{1}{4}\mathbf{D}_x^+\boldsymbol{\Lambda}_{fg}\mathbf{D}_x^-\\ -\frac{1}{4}\mathbf{D}_x^+\boldsymbol{\Lambda}_{fg}\mathbf{D}_x^- & \frac{\rho A}{k^2}\mathbf{I}-\frac{1}{4}\mathbf{D}_x^+\boldsymbol{\Lambda}_{f^2}\mathbf{D}_x^-\end{pmatrix} \tag{34}$$

$$\mathbf{b}=\begin{pmatrix}\frac{\rho A}{k^2}(2\mathbf{u}^n-\mathbf{u}^{n-1})+T_0\mathbf{D}_{xx}\mathbf{u}^n+\mathbf{D}_x^+(\boldsymbol{\psi}^{n-1/2}\circ\mathbf{g}^n)-\frac{1}{4}\mathbf{D}_x^+\boldsymbol{\Lambda}_{g^2}\mathbf{D}_x^-\mathbf{u}^{n-1}-\frac{1}{4}\mathbf{D}_x^+\boldsymbol{\Lambda}_{fg}\mathbf{D}_x^-\boldsymbol{\zeta}^{n-1}\\ \frac{\rho A}{k^2}(2\boldsymbol{\zeta}^n-\boldsymbol{\zeta}^{n-1})+T_0\mathbf{D}_{xx}\boldsymbol{\zeta}^n+\mathbf{D}_x^+(\boldsymbol{\psi}^{n-1/2}\circ\mathbf{f}^n)-\frac{1}{4}\mathbf{D}_x^+\boldsymbol{\Lambda}_{f^2}\mathbf{D}_x^-\boldsymbol{\zeta}^{n-1}-\frac{1}{4}\mathbf{D}_x^+\boldsymbol{\Lambda}_{fg}\mathbf{D}_x^-\mathbf{u}^{n-1}\end{pmatrix} \tag{35}$$

In the above, $\mathbf{D}_x^-$ is the $M \times M-1$ space derivative matrix; $\mathbf{D}_x^+ = -^T\mathbf{D}_x^-$; $\mathbf{D}_{xx}$ is the second space derivative matrix; $\mathbf{\Lambda}_v$ is the $M \times M$ diagonal matrix where the main diagonal is the vector v; $\mathbf{I}$ is the $M-1 \times M-1$ identity matrix. Also, the symbol $\circ$ denotes the element-wise product. Once $\mathbf{w}^{n+1}$ is known, one may go on and update $\boldsymbol{\psi}$ using (29). One appealing feature of both schemes (21) and (28) is that they are virtually insensitive to the choice of the potential function: in other words, the schemes leads to energy conservation regardless of the particular choice for ϕ, so long, of course, that it is positive definite, and its gradient exists and is well behaved. One attractive possibility arises as one may use the skeleton of the non-iterative scheme to test out various nonlinear potentials, effortlessly. One particularly useful potential, here, is given by the Morse and Ingard nonlinear string model, obtained as truncated series expansion of the geometrically exact case. Though conservative finite difference schemes for this particular model have been derived in the past (12), the current schemes represent a reliable tool for the analyst wishing to experiment with different models.

4 NUMERICAL EXPERIMENTS

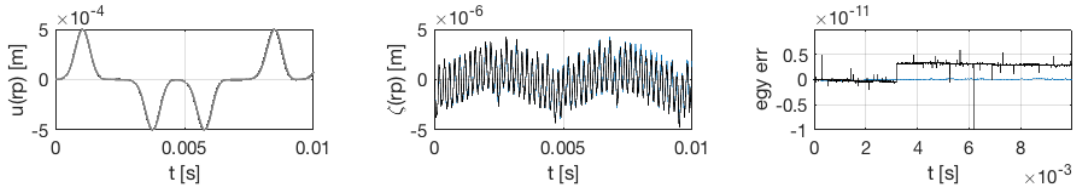

Figure 1. Low amplitude initial conditions, $U_0 = 1$ mm. The grey line is the solution obtained with the linear wave equation, the black line is the iterative nonlinear scheme, and the blue line is the proposed nonlinear non-iterative scheme. The energy error is defined as $(\mathfrak{h}^{n-1/2} - \mathfrak{h}^{1/2})/\mathfrak{h}^{1/2}$. All simulations are obtained with a sample rate $f_s = 48 \cdot 10^4$ Hz. The number of iterations for Newton-Raphson is 10.

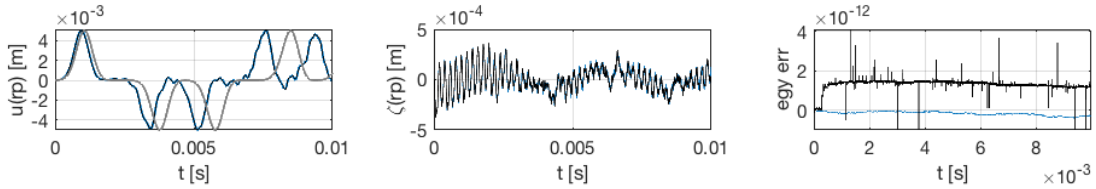

Figure 2. Medium amplitude initial conditions, $U_0 = 1$ cm. Colour scheme and sample rate as per Fig. 1.

In the following, the schemes will be compared. The simulations consider the lossless case, and initial conditions in the form of a gaussian distribution with zero initial velocity, i.e.

$$u(0,x) = U_0 e^{-\frac{(x/L+1/2)^2}{2\sigma^2}}, \qquad \partial_t u(0,x) = 0 \tag{36}$$

The free parameter U_0 (measured in metres) allows to control the level of nonlinearity in the string. In the following, $\sigma = 0.24$ will be used. The readout point is placed at $rp = 0.72L$. String parameters are selected here as so to resemble a low pitched piano string, though only for illustrative purposes. They are given as

$$L = 1 \text{ m}, \quad \rho = 8000 \text{ kg/m}^3, \quad A = 2.827 \cdot 10^{-7} \text{ m}^2, \quad T_0 = 100 \text{ N}, \quad E = 2 \cdot 10^{11} \text{ Pa} \tag{37}$$

As a first experiment, take a look at Fig. 1 and Fig. 2. As expected, under low amplitude initial conditions the output of both the iterative and of the non-iterative schemes is virtually indistinguishable from the simulation of the simple linear wave equation. As the amplitude is increased, some nonlinear effects come into existence

and as the longitudinal component becomes more prominent. Notice that energy is conserved to machine accuracy for both schemes, although some jumps are observed in the Newton-Raphson (this could be alleviated by increasing the number of iterations.)

A second experiment is considered in Fig. 3. There, high amplitude initial conditions are enforced, resulting in strongly nonlinear dynamics. Increasing the sample rate shows a gradual regularisation of the waveforms, which begin to converge to a common solution, as expected.

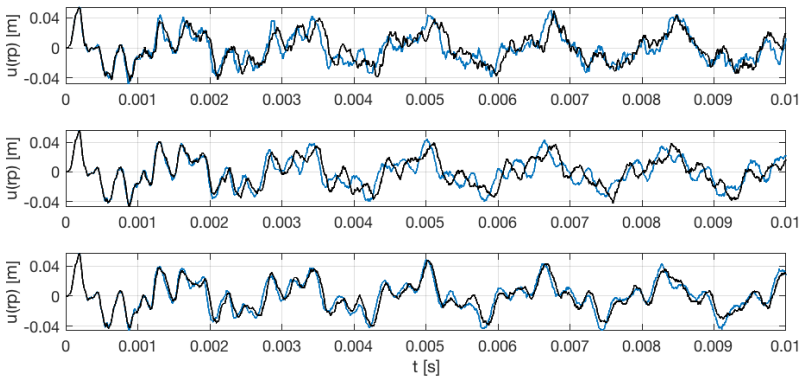

Figure 3. High amplitude initial conditions, $U_0 = 10$ cm. Top row: $f_s = 48 \cdot 10^4$ Hz, Middle Row: $f_s = 3 \cdot 48 \cdot 10^4$ Hz, Bottom Row: $f_s = 5 \cdot 48 \cdot 10^4$ Hz. Black: iterative scheme. Blue: non-iterative scheme. The number of iterations for Newton-Raphson is 10.

Finally, Fig. 4 shows the output spectra of the simulations obtained with low, medium and high amplitude initial conditions. Notice the progressive shift of the spectra away from the harmonic series predicted by linear theory.

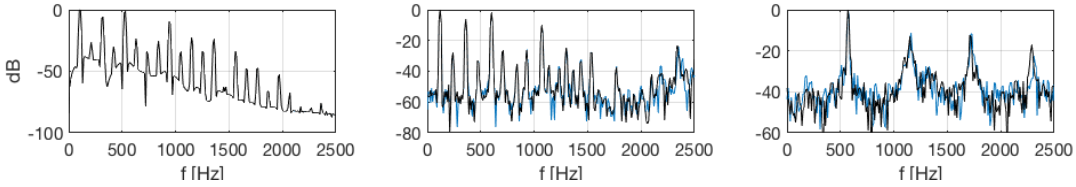

Figure 4. Output spectra of the non-iterative scheme. Left to right: $U_0 = 1$ mm, $U_0 = 1$ cm, $U_0 = 10$ cm. For all simulations $f_s = 48 \cdot 10^4$ Hz.

4.1 Computational Testing

A quick computational test was performed, on a 3.6GHz Intel core i5 CPU found in a 2011 iMac, and running Matlab R2018b. The test was run by simply recording the compute times for 0.1s of simulation. The times reported in table 1 are an average over 10 repetitions of the same simulation. It is seen that the new schemes perform much more efficiently than the iterative schemes, with speedups of about half an order of magnitude.

5 CONCLUSIONS

In this work, a novel non-iterative, conservative finite difference scheme was offered for the solution of the geometrically exact nonlinear string vibration. The new schemes are comparable to iterative schemes obtained

Table 1. Compute times for 0.1 s, under high amplitude conditions. The oversampling factor is given for a base sample rate $f_s = 48 \cdot 10^3$Hz. The iterative scheme was run with 10 iterations per time step.

Oversampling	Iterative (s)	Non-Iterative (s)	Speedup
1	3.1	0.65	4.80×
5	22.7	5.2	4.36×
10	69.3	15.5	4.47×

via the trapezoid rule in terms of resolving power, but they are much more efficient. Also, the skeleton of the scheme can be used to simulate an arbitrary nonlinear potential, provided that it is positive definite and that its gradient is well defined. These schemes follow as a particular application of emerging methods in numerical analysis, based on a quadratisation of the nonlinear potential.

ACKNOWLEDGMENTS

The first author wishes to thank the Leverhulme Trust, who is supporting his research with an Early Career Fellowship.

References

[1] A. Falaize. Modélisation, simulation, génération de code et correction de systèmes multi-physiques audios: Approche par réseau de composants et formulation hamiltonienne à ports. PhD thesis, Université Pierre et Marie Curie, Paris, July 2016.

[2] N. Lopes, T. Hélie, and A. Falaize. Explicit second-order accurate method for the passive guaranteed simulation of port-hamiltonian systems. In Proc. 5th IFAC 2015, Lyon, France, July 2015.

[3] A. Falaize and T. Hélie. Passive guaranteed simulation of analog audio circuits: A port-Hamiltonian approach. Appl. Sci., 6: 273 – 273, 2016.

[4] M. Ducceschi and S. Bilbao. Non-iterative solvers for nonlinear problems: The case of collisions. In 22nd Int. Conf. on Dig. Audio Eff. (DAFx 2019), Birmingham, UK, September 2019.

[5] S. Bilbao, M. Ducceschi, and C. Webb. A large-scale real-time modular physical modeling sound synthesis system. In 22nd Int. Conf. on Dig. Audio Eff. (DAFx 2019), Birmingham, UK, September 2019.

[6] M. Ducceschi and S. Bilbao. A physical model for the prepared piano. In Proc. 26th Int. Cong. of Sound Vib. (ICSV 2019), Montreal, Canada, July 2019.

[7] X. Yang. Linear and unconditionally energy stable schemes for the binary fluid-surfactant phase field model. Comp. Methods Appl. Mech. Eng., 318:1005–1029, 2017.

[8] J. Chabassier and S. Imperiale. Stability and dispersion analysis of improved time discretisation for prestressed Timoshenko systems. Application to the stiff piano string. Wave Motion, 50(3):456 – 480, 4 2013.

[9] M. Ducceschi and S. Bilbao. Conservative finite difference time domain schemes for the prestressed Timoshenko, shear and Euler-Bernoulli beam equations. Wave Motion, 89:142–165, 2019.

[10] A. Chaigne and J. Kergomard. Acoustics of musical instruments. Springer, New York, USA, 2016.

[11] S. Bilbao. Numerical sound synthesis: Finite difference schemes and simulation in musical acoustics. Wiley, Chichester, UK, 2009.

[12] S. Bilbao. Conservative numerical methods for nonlinear strings. J. Acoust. Soc. Am., 118:3316–3327, 2005.